Wavelet Analysis and Modeling of Time-Varying TRCs

Teck Ping Sim, and Perry Y. Li; Department of Mechanical Engineering, University of Minnesota, 11 Church Street S.E., Minneapolis, MN 55108 USA

Abstract

The tone reproduction curve (TRC) is a representation of a printer's input-output mapping for each primary color. It is a two dimensional signal with both temporal and tonal characteristics. With an appropriate signal model that represents the TRC, the entire time-varying TRC can be reconstructed from measurements of a few time-sequential scheduled print patches. The reconstructed TRC can then be used as feedback signal for control systems to compensate for any TRC variations. In the past, signal models based on Fourier basis and principal components analysis have been proposed for the design and analysis of the sampling sequence and the reconstruction filter. However, the tone reproduction has localized features in that it variation is less at some tones than at others. These features have not been exploited in previous signal models but can potentially improve the effectiveness of sampling and reconstruction algorithms. In this paper, the localized nature of wavelets is used to capture the ápriori knowledge of these local features and a wavelet based representation of the time-varying TRC is proposed. The wavelet based model is obtained from a track of experimentally obtained time-varying TRC data. The usefulness of this approach is demonstrated from the reconstruction of a time-sequentially sampled TRC.

Introduction

The tone reproduction curve (TRC) gives the printer's input to output tones mapping for each CMYK primary color separation. TRC changes with time due to disturbances in the print process such as temperature and humidity variations, material age etc. Therefore the time-varying TRC can be represented by a two-dimensional signal with a spatial (or tonal) dimension and a temporal dimension. The output of this signal is the output tones i.e.

$$y = \omega(s,t) \tag{1}$$

where $s \in [0,1]$ is the input tones, $y \in [0,1]$ is the output tones and $t \in \Re$ is time. In this paper, wavelet [1] is used to analyze and represent $\omega(s,t)$. A wavelet is a "small wave" which has its energy concentrated in time to give a tool for analysis of transient, non-stationary, or time-varying phenomenon. Unlike signal models based on Fourier basis and principal component analysis proposed in our previous work [2, 3], wavelet representation can capture the localized features of $\omega(s,t)$ in that variations is less at some tones than at others. With an effective time-varying TRC signal model, the entire time-varying TRC can be reconstructed from measurements of a few time-sequential scheduled print patches. Time-sequential sampling refers to a sampling technique where different tone samples are taken at different time instances. The reconstructed TRC can then be used as feedback control signal to compensate for any TRC variations. The use of time-sequential sampling as an effective means of sparsely sensing the time-varying TRC/CRC is reported in our previous works [2, 4, 5].

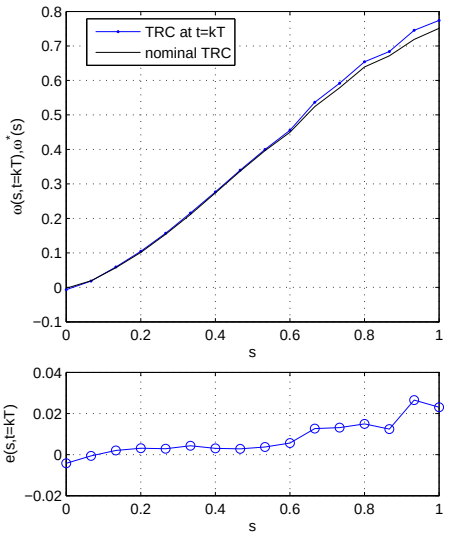

Figure 1. *An experimental TRC data of a typical xerographic printer at time-step, $t = kT$ and its variations from nominal*

The goal of this paper is therefore to use wavelet to analyze the time varying TRC and obtained a wavelet based model. The following items will be presented:

1. *Analysis:* Based on a track of experimentally obtained time-varying TRC data, wavelet analysis was conducted to determine the main *characteristics* of the two-dimensional time-varying TRC signal.
2. *Modeling:* Based on the wavelet analysis, a wavelet based model is proposed here.
3. *Demonstration:* Demonstrate the use of the wavelet based time varying TRC model to formulate an effective filter to reconstruct time-sequentially sampled TRC.

Wavelet Analysis of Time-Varying TRC

Figure 1 shows the TRC and its error from nominal at a particular time-step, $t = kT$ for $s \in \{0, \frac{1}{15}, \frac{2}{15}, \ldots, 1\}$. The error is defined here as:

$$e(s,t = kT) = \omega(s,kT) - \omega^*(s) \tag{2}$$

where $\omega^*(s)$ is the nominal TRC. Figure 2 shows the 16 output tones at different time-step, k for a track of experimental TRC data. Note that the variations of the output tones depends on the

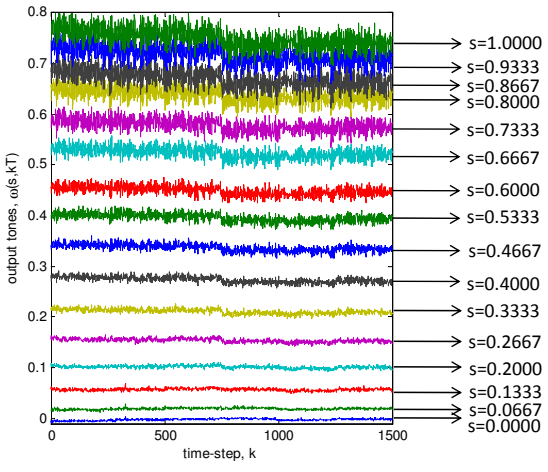

Figure 2. *Time-varying TRC for cyan with continuous measurement of 1500 prints printed at 60ppm*

input tones, $s \in [0,1]$. In addition it is expected that the time varying TRC have different time scale of variations e.g. the photoreceptor which degrades with time results in much slower changes in printout compare to the effects of changes in environmental factors, etc. These localized variations motivate the use of wavelet for representing the time-varying TRC.

In wavelet analysis, any function, $f(x) \in \mathscr{L}^2(\Re)$ can be written as:

$$f(x) = \sum_{\ell} c_{j_0}(\ell) 2^{j_0/2} \varphi(2^{j_0}x - \ell) + \sum_{j=j_0}^{\infty} \sum_{\ell} d_j(\ell) 2^{j/2} \psi(2^j x - \ell) \tag{3}$$

where $\varphi(\cdot)$ and $\psi(\cdot)$ is the scaling and wavelet functions respectively. j_0 can be set to any integer value. The choice of j_0 sets the coarsest scale whose space is spanned by $2^{j_0/2}\varphi(2^{j_0}x-\ell)$. The rest of $\mathscr{L}^2(\Re)$ is spanned by the wavelets which provide the high resolution details of the signal. In practice since only the samples of a signal is given, there is a highest resolution when the finest scale is at the sample level i.e. j has a finite upper value. See [1] for details on wavelets.

Since there are only 16 data samples, the highest scale achievable is $J = 4$ (corresponding to $2^J = 16$). With $j_0 = 0$ and $s \in [0,1]$, (3) can be simplified and rewritten for $e(s,kT)$ of equation (2) as:

$$e(s,kT) = c_0\varphi(s) + \sum_{j=0}^{J-1} \sum_{\ell=0}^{2^j-1} d_j(\ell) 2^{j/2} \psi(2^j s - \ell) \tag{4}$$

Figure 3 shows this decomposition using the Haar wavelet [1]. At the scaling level and each j wavelet scale level there are the scaling and wavelet coefficients i.e. $[c_0]$, $[d_0(0)]$, $[d_1(0), d_1(1)]$, $[d_2(0), d_2(1), d_2(2), d_2(3)]$, and $[d_3(0), d_3(1), \ldots, d_3(7)]$. Let this set of coefficients be given by:

$$\rho := \left[\begin{array}{c} c_0, d_0(0), d_1(0), d_1(1), d_2(0), d_2(1), d_2(2), d_2(3), \\ d_3(0), d_3(1), \ldots, d_3(7) \end{array} \right]^T \tag{5}$$

Henceforth let ρ be known as the tonal wavelet coefficients. At

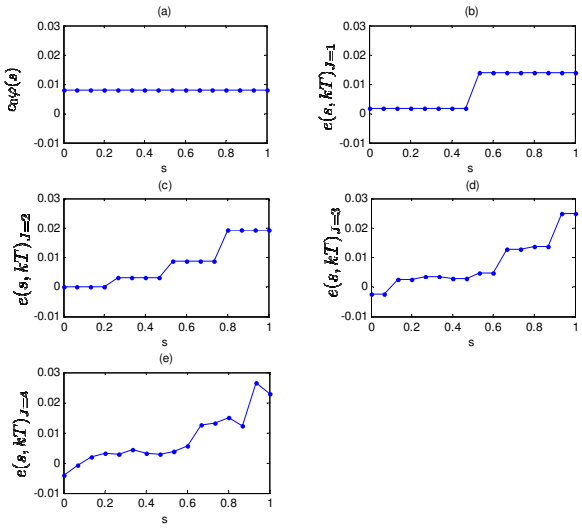

Figure 3. *(a) signal approximation at scaling level; (b) signal approximation at scaling level and wavelet details at scale $j = 0$; (c) signal approximation at scaling level and wavelet details at scale up to $j = 1$; (d) signal approximation at scaling level and wavelet details at scale up to $j = 2$; (e) signal approximation at scaling level and wavelet details at scale up to $j = 3$*

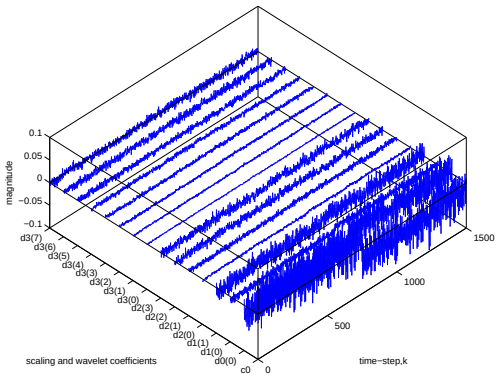

Figure 4. *Magnitude of scaling and wavelet coefficients at all time-steps, k.*

each time-step, $t = kT$, there is a new set of tonal wavelet coefficients. Figure 4 shows these coefficients at all time-step. To analyze the temporal properties of the signal, we looked into the variations of the wavelet coefficients. For example, lets consider the c_0 coefficient. Performing a 3-levels wavelet analysis on c_0 we have from equation (3) (using $\bar{c}_0(\ell)$ and $\bar{d}_j(\ell)$ as representation of the new wavelet coefficients set) represent c_0 as.

$$c_0 := \rho(1,kT) = \underbrace{\sum_{\ell} \bar{c}_0(\ell)\varphi(kT-\ell)}_{{}^1\alpha_3(k)} + \underbrace{\sum_{j=0}^{2} \sum_{\ell} \bar{d}_j(\ell) 2^{j/2} \psi(2^j kT - \ell)}_{\sum_{j=1}^{3} {}^1\delta_j(k)} \tag{6}$$

where ${}^1\delta_j(k) = \sum_{\ell} \bar{d}_{3-j}(\ell) 2^{(3-j)/2} \psi(2^{(3-j)}kT - \ell)$. Figure 5 shows the wavelet analysis for $\rho(1,kT)$ using the Symlet-4

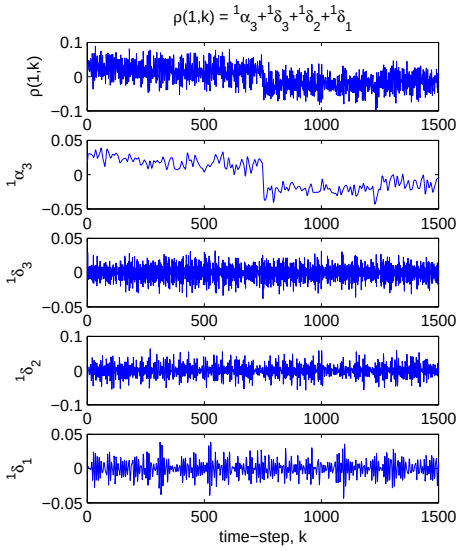

Figure 5. *Temporal wavelet decomposition of the scaling coefficients c_0 using Symlet-4 wavelet.*

wavelet. The frequency contents at each level of the decomposition are shown in Figure 6 which is clearly separated into different frequency sub-bands - a distinct low-pass band for ${}^1\alpha_3(k)$, band-pass bands for ${}^1\delta_3(k)$ and ${}^1\delta_2(k)$ and a high-pass band for ${}^1\delta_1(k)$.

Wavelet Based Model for Time-Varying TRC

From (4), (5) and for $J=4$ with $M=16$ sample points we have:

$$\underbrace{\begin{pmatrix} e(s_0,kT) \\ \vdots \\ e(s_{15},kT) \end{pmatrix}}_{\mathbf{e}(k)} = \underbrace{\begin{pmatrix} \varphi(s_0) & \psi_{0,0}(s_0) & \cdots & \psi_{3,7}(s_0) \\ \vdots & \vdots & \ddots & \vdots \\ \varphi(s_{15}) & \psi_{0,0}(s_{15}) & \cdots & \psi_{3,7}(s_{15}) \end{pmatrix}}_{\Gamma} \rho(k) \tag{7}$$

where $\psi_{j,\ell}(x) := 2^{j/2}\psi(2^j x-\ell)$ and Γ gives the wavelet basis matrix. Generalizing the temporal wavelet analysis on the tonal wavelet coefficient as given by equation (6), we have:

$$\rho(i,k) = {}^i\alpha_3(k) + \sum_{j=1}^{3} {}^i\delta_j(k), \text{ for } i=1,2,\ldots,I=\sum_{r=0}^{J-1} 2^r \tag{8}$$

where the signals from the wavelet decomposition can be represented by a pink noise sequence with appropriate cutoff frequencies and covariance settings i.e.:

$$\begin{aligned} {}^i\xi_{\alpha_3}(k+1) &= {}^i\mathbf{A}_{\alpha_3}{}^i\xi_{\alpha_3}(k) + {}^i\mathbf{B}_{\alpha_3}{}^i\mathbf{w}_{\alpha_3}(k) & (9)\\ {}^i\alpha_3(k) &= {}^i\mathbf{C}_{\alpha_3}{}^i\xi_{\alpha_3}(k) + {}^i\mathbf{D}_{\alpha_3}{}^i\mathbf{w}_{\alpha_3}(k) & (10)\end{aligned}$$

$({}^i\mathbf{A}_{\alpha_3}, {}^i\mathbf{B}_{\alpha_3}, {}^i\mathbf{C}_{\alpha_3}, {}^i\mathbf{D}_{\alpha_3})$ are obtained from a n-th order Butterworth filter with the low-pass cutoff frequency and ${}^i\mathbf{w}_{\alpha_3}(k) \sim N(0, {}^i\mathbf{Q}_{\alpha_3})$. Similarly, for $j=1,2$ and, 3 we have:

$$\begin{aligned} {}^i\xi_{\delta_j}(k+1) &= {}^i\mathbf{A}_{\delta_j}{}^i\xi_{\delta_j}(k) + {}^i\mathbf{B}_{\delta_j}{}^i\mathbf{w}_{\delta_j}(k) & (11)\\ {}^i\delta_j(k) &= {}^i\mathbf{C}_{\delta_j}{}^i\xi_{\delta_j}(k) + {}^i\mathbf{D}_{\delta_j}{}^i\mathbf{w}_{\delta_j}(k) & (12)\end{aligned}$$

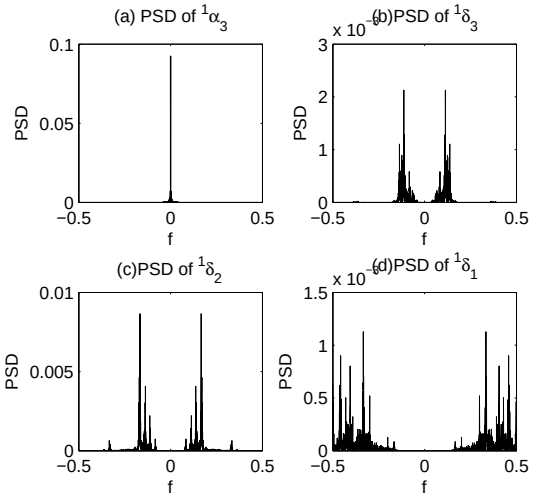

Figure 6. *Frequency content (power spectral density) of the temporal wavelet decomposition of the spatial scaling coefficients c_0. (a) frequency content of the low-pass band for signal ${}^1\alpha_3$ with cutoff frequency of 0.005 Hz and covariance of 9.47×10^{-2} ; (b) frequency content of the band-pass band for signal ${}^1\delta_3$ with cutoff frequencies of [0.05,0.15] Hz and covariance of 1.04×10^{-2} ; (c) frequency content of the band-pass band for signal ${}^1\delta_2$ with cutoff frequencies of [0.075,0.18] Hz and covariance of 2.20×10^{-2} ; (d) frequency content of the high-pass band for signal ${}^1\delta_1$ with cutoff frequency of 0.31 Hz and covariance of 1.31×10^{-2}*

$({}^i\mathbf{A}_{\delta_j}, {}^i\mathbf{B}_{\delta_j}, {}^i\mathbf{C}_{\delta_j}, {}^i\mathbf{D}_{\delta_j})$ are obtained from a n-th order Butterworth filter with the appropriate cutoff frequencies and ${}^i\mathbf{w}_{\delta_j}(k) \sim N(0, {}^i\mathbf{Q}_{\delta_j})$. The cut-off frequencies and covariance matrices of each of the n-th order Butterworth filter that model the sub-bands can be obtained from the wavelet analysis as shown in Figure 6 for $i=1$. Let ${}^i\bar{\xi}(k) := [{}^i\xi_{\alpha_3}, {}^i\xi_{\delta_3}, {}^i\xi_{\delta_2}, {}^i\xi_{\delta_1}]^T$ and ${}^i\bar{\mathbf{w}}(k) := [{}^i\mathbf{w}_{\alpha_3}, {}^i\mathbf{w}_{\delta_3}, {}^i\mathbf{w}_{\delta_2}, {}^i\mathbf{w}_{\delta_1}]^T$, then equations 8-12 can be rewritten as:

$$\begin{aligned} \rho(i,k) &= \underbrace{\begin{pmatrix} {}^i\mathbf{C}_{\alpha_3} & {}^i\mathbf{C}_{\delta_3} & {}^i\mathbf{C}_{\delta_2} & {}^i\mathbf{C}_{\delta_1} \end{pmatrix}}_{{}^i\bar{\mathbf{C}}} {}^i\bar{\xi}(k) \\ &+ \underbrace{\begin{pmatrix} {}^i\mathbf{D}_{\alpha_3} & {}^i\mathbf{D}_{\delta_3} & {}^i\mathbf{D}_{\delta_2} & {}^i\mathbf{D}_{\delta_1} \end{pmatrix}}_{{}^i\bar{\mathbf{D}}} {}^i\bar{\mathbf{w}}(k) & (13)\\ {}^i\bar{\xi}(k+1) &= {}^i\bar{\mathbf{A}}{}^i\bar{\xi}(k) + {}^i\bar{\mathbf{B}}{}^i\bar{\mathbf{w}}(k) & (14)\end{aligned}$$

Let $\rho(k) := [\rho(1,k), \rho(2,k), \ldots, \rho(I,k)]^T$, we can concatenate (13) and (14) to yield the following equations:

$$\begin{aligned} \rho(k) &= \bar{\mathbf{C}}\bar{\xi}(k) + \bar{\mathbf{D}}\bar{\mathbf{w}}(k) & (15)\\ \bar{\xi}(k+1) &= \bar{\mathbf{A}}\bar{\xi}(k) + \bar{\mathbf{B}}\bar{\mathbf{w}}(k) & (16)\end{aligned}$$

where $\bar{\mathbf{A}} := \text{diag}({}^1\bar{\mathbf{A}}, \ldots, {}^I\bar{\mathbf{A}})$, $\bar{\mathbf{B}} := \text{diag}({}^1\bar{\mathbf{B}}, \ldots, {}^I\bar{\mathbf{B}})$, $\bar{\mathbf{C}} := \text{diag}({}^1\bar{\mathbf{C}}, \ldots, {}^I\bar{\mathbf{C}})$, $\bar{\mathbf{D}} := \text{diag}({}^1\bar{\mathbf{D}}, \ldots, {}^I\bar{\mathbf{D}})$, $\bar{\xi}(k) := [{}^1\bar{\xi}(k), {}^2\bar{\xi}(k), \ldots, {}^I\bar{\xi}(k)]^T$ and $\bar{\mathbf{w}}(k) := [{}^1\bar{\mathbf{w}}(k), {}^2\bar{\mathbf{w}}(k), \ldots, {}^I\bar{\mathbf{w}}(k)]^T$. Substituting (15) into (7) we have:

$$\mathbf{e}(k) = \Gamma\bar{\mathbf{C}}\bar{\xi}(k) + \Gamma\bar{\mathbf{D}}\bar{\mathbf{w}}(k) \tag{17}$$

Equations (16) and (17) give the wavelet based print variations model. This model gives a more rigorous model for modeling

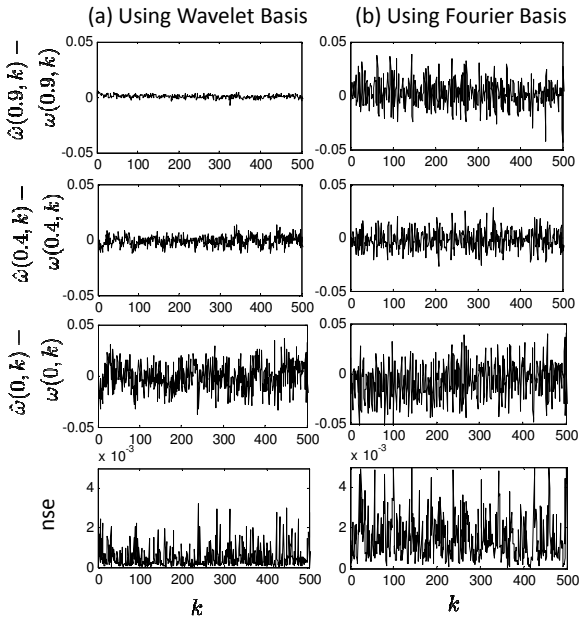

Figure 7. *Sparse sensing of an experimental track of time-varying TRC using the optimized time-sequential sampling and reconstruction filter using the (a) proposed wavelet based model and (b) Fourier based model proposed in our previous work. Top three figures show the errors between the reconstructed and actual TRC at three different input tones - 0%,40% and 90%. Bottom most figure shows the norm squared of reconstructed and actual TRC errors.*

the TRC variations. In the next section we demonstrate the effectiveness of using the wavelet-based TRC variations model in reconstructing time-sequential sampled signals.

Use of Wavelet Based Model for Reconstructing Time-Sequential Sampled Signal

The wavelet based model of the time-varying TRC is used here as the basis for a reconstruction filter of time-sequentially sampled signal. Time-sequential sampling refers to a sampling technique where different tone samples are taken at different time instances. To recover the complete TRC signal from these time-sequentially sampled tones, a reconstruction filter using a periodic Kalman filter was proposed in [2]. Effectiveness of this filter to recover the TRC depends on the time-sequential sampling design and the time-varying TRC model. The former was addressed using the optimized time-sequential sampling design in the lattice framework [6, 7]. The latter was addressed in this paper using the wavelet based model, that accounts for important localized variations of the TRC.

Figure 7(a) shows the results of using this model based on the identified parameters given through the wavelet signal analysis for reconstructing the time-sequentially sampled signal. The result clearly shows much better reconstruction performance compared to the Fourier based model proposed in our previous work [2] as shown in Figure 7(b). Hence, the use of the wavelet based model improves the fidelity of the TRC reconstruction.

Conclusion

The experimental track of time-varying TRC shows that this signal class contains both localized tonal and temporal features. This motivates the use of wavelet descriptors since wavelet basis are localized. Wavelet gives a cohesive framework to analyze and represent the time-varying TRC. In paper we show that the time-varying TRC can be effectively represented using wavelet coefficients to capture the *àpriori* knowledge of local features. The wavelet representation is shown to give high fidelity reconstruction of time-sequentially sampled tones. In addition, the wavelet framework enables extension to analyze and represent the time-varying color reproduction characteristics (CRC) function.

Acknowledgment

This research is supported by Ricoh Company of Japan in collaboration with Dr. Takashi Yamaguchi and Dr. Hirobumi Nishida of Ricoh's Core Technology R&D Center, Yokohama, Japan. Their inputs are gratefully acknowledged.

References

[1] C.S.Burrus, T.A. Gopinath and H. Guo, Introduction to wavelets and wavelet transforms, Prentice-Hall (1998).

[2] T.P.Sim, P.Y.Li and D.J.Lee, Using time-sequential sampling to stabilize the color and tone reproduction functions of a xerographic printing process, IEEE Transactions on Control Systems Technology, 15(2), 349 (2007).

[3] T.P.Sim, Sensing and Control for Color Consistency of the Xerographic Printing Process, Ph.D. thesis, University of Minnesota (2009).

[4] T.P.Sim and P.Y.Li, Stabilization of color/tone reproduction curves using time-sequential sampling, in Non-Impact Printing 20, IS&T, Salt Lake City, pp. 204–209 (2004).

[5] T.P.Sim and P.Y.Li, Direct color consistency control for xerographic printing, in Non-Impact Printing 25, IS&T, Louisville, pp. 678–681 (2009).

[6] T.P.Sim and P.Y.Li, Optimal time sequential sampling of tone reproduction function, in American Control Conference ACC, IEEE, Minneapolis, United States, pp. 5728–5733 (2006).

[7] T.P.Sim and P.Y.Li, Optimal time-sequential sampling of color reproduction characteristic function, in Non-Impact Printing 22, IS&T, Denver, pp. 585–591 (2006).

Author Biography

Teck Ping, Sim received the Ph.D degree in Mechanical Engineering from the University of Minnesota, Twin Cities, MN in 2009. From 2009-2010, he was a postdoctoral associate at the University of Minnesota working on a collaborative project with Ricoh Co. of Japan. Since 2010 he works with E-Ink Corporation at Cambridge, MA. His research interests are in control systems and signal processing as applied to imaging systems and robotics.

Perry Y. Li received the Ph.D degree in Mechanical Engineering for the University of California, Berkeley in1995. From 1995-1997, he was a research staff at Xerox Corporation, Webster, NY. He has been with the University of Minnesota since 1997 and is currently Professor of Mechanical Engineering. His research interests are in mechatronics and controls systems as applied to fluid power, robotics, and imaging systems.